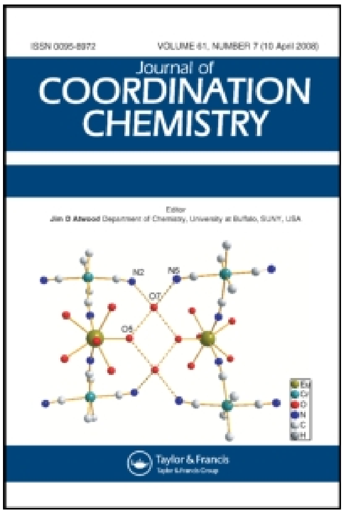

Journal of Coordination Chemistry
Publication details, including instructions for authors and subscription information:
http://www.informaworld.com/smpp/title~content=t713455674

Mono-Sulfonated Derivatives of Triphenylphosphine, $[NH_4]$TPPMS and $M(TPPMS)_2$ (TPPMS = $P(Ph)_2(m\text{-}C_6H_4SO_3^-)$; M = Mn^{2+}, Fe^{2+}, Co^{2+} and Ni^{2+}). Crystal Structure Determinations for $[NH_4][TPPMS]\cdot½H_2O$, $[Fe(H_2O)_5(TPPMS)]$TPPMS, $[Co(H_2O)_5TPPMS]$TPPMS and $[Ni(H_2O)_6](TPPMS)_4\cdot H_2O$

Mark R. Barton[a]; Yuegang Zhang[a]; Jim D. Atwood[a]
[a] Department of Chemistry, University at Buffalo, State University of New York, Buffalo, NY, USA

Online publication date: 15 September 2010

To cite this Article Barton, Mark R. , Zhang, Yuegang and Atwood, Jim D.(2002) 'Mono-Sulfonated Derivatives of Triphenylphosphine, $[NH_4]$TPPMS and $M(TPPMS)_2$ (TPPMS = $P(Ph)_2(m\text{-}C_6H_4SO_3^-)$; M = Mn^{2+}, Fe^{2+}, Co^{2+} and Ni^{2+}). Crystal Structure Determinations for $[NH_4][TPPMS]\cdot½H_2O$, $[Fe(H_2O)_5(TPPMS)]$TPPMS, $[Co(H_2O)_5TPPMS]$TPPMS and $[Ni(H_2O)_6](TPPMS)_4\cdot H_2O$', Journal of Coordination Chemistry, 55: 8, 969 — 983
To link to this Article: DOI: 10.1080/0095897022000002295
URL: http://dx.doi.org/10.1080/0095897022000002295

PLEASE SCROLL DOWN FOR ARTICLE

J. Coord. Chem., 2002, Vol. 55(8), pp. 969–983

MONO-SULFONATED DERIVATIVES OF TRIPHENYLPHOSPHINE, $[NH_4]$TPPMS AND $M(TPPMS)_2$ (TPPMS = $P(Ph)_2(m\text{-}C_6H_4SO_3^-)$; M = Mn^{2+}, Fe^{2+}, Co^{2+} AND Ni^{2+}). CRYSTAL STRUCTURE DETERMINATIONS FOR $[NH_4][TPPMS]\cdot\frac{1}{2}H_2O$, $[Fe(H_2O)_5(TPPMS)]TPPMS$, $[Co(H_2O)_5TPPMS]TPPMS$ AND $[Ni(H_2O)_6](TPPMS)_2\cdot H_2O$

MARK R. BARTON, YUEGANG ZHANG and JIM D. ATWOOD*

Department of Chemistry, University at Buffalo, State University of New York at Buffalo, Natural Science Complex, Buffalo, NY 14260-3000, USA

(Received 31 August 2001; Revised 11 September 2001; In final form 01 November 2001)

Preparation of the ammonium salt of TPPMS, $[NH_4]$TPPMS, TPPMS = $PPh_2(m\text{-}C_6H_4SO_3^-)$, greatly enhances water solubility and provides an efficient route to other metal complexes of TPPMS, $M(TPPMS)_2$ M = Mn^{2+}, Co^{2+}, Fe^{2+} and Ni^{2+}. For Co^{2+} and Fe^{2+} the metal has an octahedral ligand environment with five water molecules and one TPPMS coordinated through the sulfonate oxygen; the second TPPMS is not coordinated. For Ni^{2+} the octahedral coordination sphere is composed of water molecules and the TPPMS ligands are not coordinated. Structures are fully reported for $[NH_4]TPPMS\cdot\frac{1}{2}H_2O$ and $[Fe(H_2O)_5(TPPMS)]TPPMS$ and partially reported for $[Co(H_2O)_5TPPMS]TPPMS$ and $[Ni(H_2O)_6]TPPMS_2\cdot H_2O$. All of the structures show hydrophobic regions consisting of aromatic rings and hydrophilic regions with hydrogen-bonding interactions.

Keywords: Water-soluble phosphine ligands; TPPMS; Hydrophilic interaction; Coordination complexes

INTRODUCTION

Research in the field of water-soluble organometallic chemistry continues to intensify forty-two years after the initial synthesis of a water-soluble phosphine [1] (sodium diphenylphosphinobenzene-*m*-sulfonate) **1**. Rhone-Poluenc/Ruhrchemie's use of the hydroformylation catalyst, $HRh(CO)L_3$, where L = trisodium tris(3-sulfonatophenyl) phosphine, **3**, for over a quarter-century [2,3] has fueled increasing interest.

*Corresponding author. Tel.: 716 645 6800 ext. 2127. Fax: 716 645 6963. E-mail: jatwood@acsu.buffalo.edu

ISSN 0095-8972 print: ISSN 1029-0387 online © 2002 Taylor & Francis Ltd
DOI: 10.1080/0095897022000002295

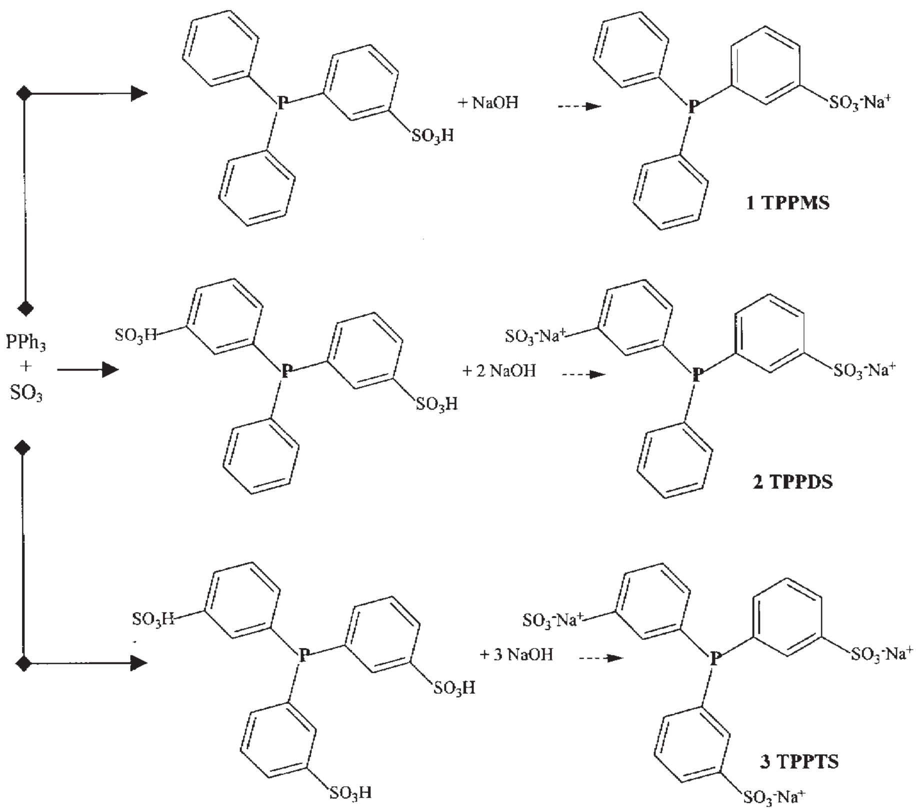

SCHEME 1

Numerous syntheses and review articles [4,5] have been published. Two commonly used water-soluble ligands, **1** and **3**, are prepared by the sulfonation of triphenylphosphine (Scheme 1).

In this report, the traditional abbreviations of TPPMS, TPPDS and TPPTS are modified to include the cation, i.e. NaTPPMS, Na_2TPPDS and Na_3TPPTS. The ligand Na_3TPPTS has been cited frequently in the recent literature, due to its solubility of 1100 g/L in water at room temperature [6]. NaTPPMS has a reported water-solubility range from 12 [7] to 80 g/L [3] at room temperature. We have found the solubility to be 28 g/L at ambient conditions.

The trade-off for the marked increase in solubility of Na_3TPPTS is a greater propensity toward oxidation in water [8]. There is also a modest electronic difference (see Fig. 1) and increased steric bulk. An effective cone angle for NaTPPMS can be obtained from literature values for PPh_3 (145.0°) [9] and Na_3TPPTS (165.6°) [10] using Tolman's method [9], where the cone angle for unsymmetrical ligands is a statistical average of its components from symmetrical analogs. Therefore, NaTPPMS has a theoretical cone angle of 151.9°. The phosphorus-substituent bond angle affects phosphine basicity [9]. The nonbonding pair on PR_3 increases *p* character and loses *s* character as the CPC angle increases. Ligand function may be altered by more than steric and electronic differences as shown by Darensbourg and Bischoff [10] who

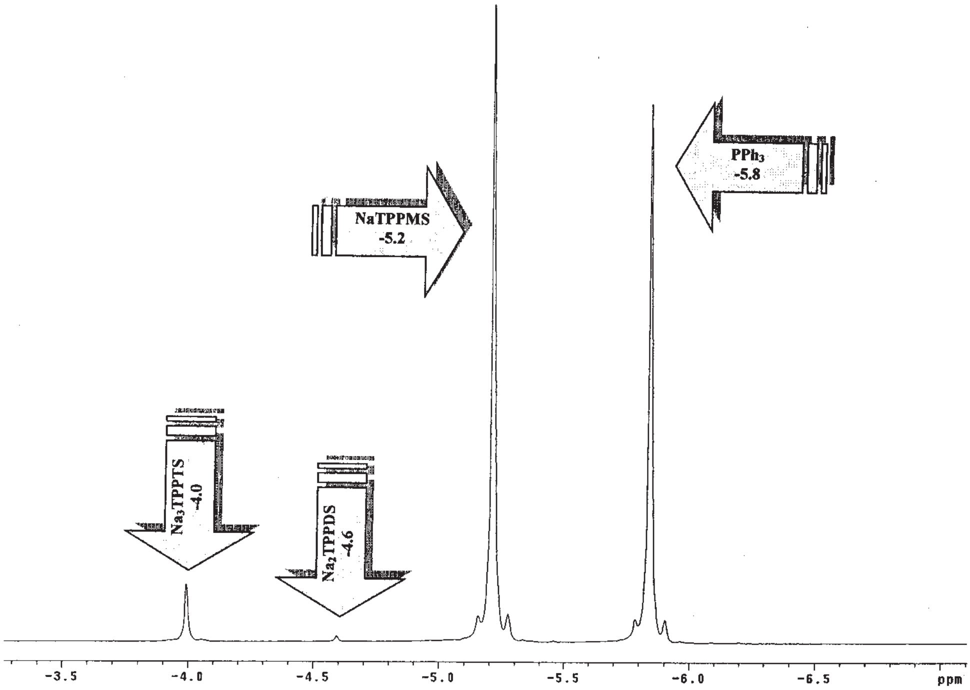

FIGURE 1 ^{31}P NMR shift comparison of PPh_3, NaTPPMS, Na_2TPPDS, and Na_3TPPTS in d_6-DMSO.

noted an intramolecular interligand stabilization during ligand substitution reactions. The rate of substitution was *cis*-$Mo(CO)_4(PPh_3)_2$ > *cis*-$Mo(CO)_4(Na_3TPPTS)_2$, attributed to slower dissociation of *cis*-$Mo(CO)_4(Na_3TPPTS)_2$ from sodium-sulfonate bonding.

This paper reports modification to the synthesis of NaTPPMS reported by Joo *et al.* [11] improving product yield, solubility (ammonium cation), and ease of synthesis. Additionally, syntheses for $Mn(TPPMS)_2$, $Fe(TPPMS)_2$, $Co(TPPMS)_2$ and $Ni(TPPMS)_2$ and crystal structures of NH_4TPPMS, $Fe(TPPMS)_2$, $Co(TPPMS)_2$ and $Ni(TPPMS)_2$ are presented.

EXPERIMENTAL

Materials and Methods

Reactions were performed under ambient conditions unless otherwise stated. Water was triply distilled and all other solvents were used as received. Deuterium oxide was purchased from Isotec, Inc. DMSO-d_6 was obtained from Aldrich. K_2PtCl_4 and $H_2PtCl_6 \cdot 6H_2O$ were purchased from Strem Chemicals and used as received. All other reagents were obtained from commercial sources and used as received. $PtCl_2$ was prepared by published procedures [18].

^1H NMR (400 MHz) and $^{31}P\{^1H\}$NMR were recorded on a Varian XL 400 spectrometer. ^{31}P NMR spectra were measured at 161.9 MHz and referenced to an external standard of 85% H_3PO_4 in D_2O set at 0.00 ppm. Analyses were performed by E and R Microanalytical Laboratory in Parsipanny, NJ. Most pH measurements used a Fisher Scientific Accumet pH meter with a glass pH electrode (silver/silver chloride reference). Indicator paper with a ± 1 pH unit (0–14 range) was used to measure pH during neutralization. Melting points were obtained using a Mel-Temp by Laboratory Devices. DSC was performed on a Perkin-Elmer 7 series thermal analysis system.

NH_4TPPMS A volume of 50 mL of 20% fuming H_2SO_4 was placed into a 150 mL Erlenmeyer flask with stir bean and cooled to $\sim 15°C$. A mass of finely ground PPh_3 20.0 g is slowly added over 40–50 min. After dissolution, the flask was heated at 98°C for another 70 min. The flask was cooled to room temperature and the contents were slowly poured over 300 g of ice in a 1.0-L beaker. The temperature was lowered to 10°C and maintained below 10°C during slow neutralization with 118 mL of concentrated aqueous ammonia. Precipitation occurred at a pH of ~ 0 and continued as more ammonia was added. The neutralization was terminated at pH 4. After filtration and 8 h drying *in vacuo*, 13.3 g (44.6%) of white powder was obtained. The melting point range was 224–228°C. Differential scanning calorimetry (DSC) indicated a m.p. onset of 226.8°C. $^{31}P\{^1H\}$ (D_2O) δ (ppm) -5.2 (s) Anal. Calcd. for NH_4TPPMS: C 60.16, H 5.05, N 3.90; found C 59.87, H 5.17, N 3.88.

NaTPPMS Na_2SO_4 (0.31 g) (2.2 mmole) was dissolved in 0.75 mL warm water. The Na_2SO_4(aq) was transferred to a warm solution of NH_4TPPMS(aq) [0.6096 g (1.7 mmol)/2.0 mL]. Both solutions are near their solubility limits. After the precipitation commenced, the mixture was allowed to cool. Filtration and drying *in vacuo* produced 0.5304 g (86%) of shiny "mica-like" flakes. M.p. 224–226°C, $^{31}P\{^1H\}$(D_2O) δ (ppm) -5.5 (s) Anal. Calcd. for NaTPPMS $\cdot$ 1.5H_2O: C 55.24, H 4.38; found C 55.14, H 4.17.

Mn(TPPMS)$_2$, Fe(TPPMS)$_2$, Co(TPPMS)$_2$, Ni(TPPMS)$_2$ The metathesis procedure described for NaTPPMS was followed for each transition metal salt. Approximately 0.65 mmol of $MSO_4 \cdot nH_2O$ was dissolved in a minimal amount of H_2O. Subsequently, the salt solution was added to 1.0 mmol [NH_4]TPPMS(aq). The ppt was filtered and dried *in vacuo*.

Mn(TPPMS)$_2$ Recovered 0.3472 g (93%), off-white flakes, $^{31}P\{^1H\}$(DMSO-d_6) δ (ppm) -1.3 broad (s) Anal. Calcd. for Mn(TPPMS)$_2 \cdot 4H_2O$: C 53.40, H 4.48; found C 53.21, H 4.30.

Fe(TPPMS)$_2$ Recovered 0.3493 g (91%), pink flakes, $^{31}P\{^1H\}$(DMSO-d_6) δ (ppm) -1.5 broad (s) Anal. Calcd. for Fe(TPPMS)$_2 \cdot 5H_2O$: C 52.18, H 4.62; found C 51.92, H 4.05.

Co(TPPMS)$_2$ Recovered 0.3117 g (81%), off-white flakes, $^{31}P\{^1H\}$(DMSO-d_6) δ (ppm) -4.5 broad (s) Anal. Calcd. for Co(TPPMS)$_2 \cdot 5H_2O$: C 51.99, H 4.61; found C 52.13, H 4.62.

Ni(TPPMS)$_2$ Recovered 0.3058 g (79%), light-green flakes, $^{31}P\{^1H\}$(DMSO-d_6) δ (ppm) -5.0 broad (s) Anal. Calcd. for Ni(TPPMS)$_2 \cdot 5H_2O$: C 52.01, H 4.61; found

C 52.02, H 4.48. The compound decomposes at 263–265°C in air, but changed color to yellow at 125°C.

[PtClL$_3$]Cl, L = NH_4^+, Mn^{2+}, Fe^{2+}, Co^{2+}, Ni^{2+} (TPPMS). Made *in situ*: four equivalents of L to one equivalent of $PtCl_2$ (0.0014 g) in 250 μl D_2O, heated to 80°C for 20 min.

NH_4^+: $^{31}P\{^1H\}$(D_2O @ 50°C) δ (ppm): 23.3 (d) ($^2J_{P\text{–}P}$ = 18.7 Hz, $^1J_{P\text{–}Pt}$ = 2500 Hz, P *trans* to P), 12.6 (t) ($^2J_{P\text{–}P}$ = 18.7 Hz, $^1J_{P\text{–}Pt}$ = 3600 Hz, P *trans* to Cl), − 5.2 (s)
Mn^{2+}: $^{31}P\{^1H\}$(D_2O @ 50°C) δ (ppm): 23.2 (d) ($^2J_{P\text{–}P}$ = 18.7 Hz, $^1J_{P\text{–}Pt}$ = 2500 Hz, P *trans* to P), 12.4 (t) ($^2J_{P\text{–}P}$ = 18.7 Hz, $^1J_{P\text{–}Pt}$ = 3600 Hz, P *trans* to Cl), − 4.7 broad
Fe^{2+}: $^{31}P\{^1H\}$(D_2O @ 50°C) δ (ppm): 23.1 (d) ($^2J_{P\text{–}P}$ = 18.7 Hz, $^1J_{P\text{–}Pt}$ = 2500 Hz, P *trans* to P), 12.3 (t) ($^2J_{P\text{–}P}$ = 18.7 Hz, $^1J_{P\text{–}Pt}$ = 3600 Hz, P *trans* to Cl), − 2.8 broad
Co^{2+}: $^{31}P\{^1H\}$(D_2O @ 50°C) δ (ppm): 23.1 (d) ($^2J_{P\text{–}P}$ = 18.7 Hz, $^1J_{P\text{–}Pt}$ = 2500 Hz, P *trans* to P), 12.3 (t) ($^2J_{P\text{–}P}$ = 18.7 Hz, $^1J_{P\text{–}Pt}$ = 3600 Hz, P *trans* to Cl), − 1.9 broad
Ni^{2+}: $^{31}P\{^1H\}$(D_2O @ 50°C) δ (ppm): 23.3 (d) ($^2J_{P\text{–}P}$ = 18.7 Hz, $^1J_{P\text{–}Pt}$ = 2500 Hz, P *trans* to P), 12.6 (t) ($^2J_{P\text{–}P}$ = 18.7 Hz, $^1J_{P\text{–}Pt}$ = 3600 Hz, P *trans* to Cl), − 4.0 broad

Crystal Structures of NH_4TPPMS · ½H_2O and Fe(TPPMS)$_2$ · 5H_2O Colorless prism shape crystals of NH_4TPPMS · ½H_2O were grown by slow evaporation of an aqueous solution, while yellow needles of Fe(TPPMS)$_2$ · 5H_2O were grown by slowly cooling a hot, aqueous solution in a Dewar flask. X-ray diffraction data were collected with the SMART program [19] on a Brucker SMART 1000 CCD diffractometer at 90(1) K installed at a rotating anode (Mo Kα radiation λ = 0.71071 Å) source, and equipped with an LN_2 Oxford Cryostream Cooler. A mounted crystal was immediately placed into the nitrogen stream to avoid possible loss of solvent of crystallization. The program SAINT was used for integration of the diffraction profiles [20]. The structures were determined by Patterson methods using SHELXS program in SHELXTL package [21]. The structure was refined with SHEXL and hydrogen atoms attached to carbon atoms were placed in calculated positions. All of the non-hydrogen atoms were refined anisotropically. There exists racemic twinning in the Fe(TPPMS)$_2$ · 5H_2O structure. Structural graphics were provided by SHELXP and Weblab Viewer [22] for Windows.

RESULTS AND DISCUSSION

A limitation to the use of TPPMS is the relatively low solubility in comparison to TPPTS. Our measurements under comparable conditions show the solubilities to be Na_3TPPTS, 1100 g/L; NaTPPMS, 28 g/L; and KTPPMS, 12 g/L. Frequently metal complexes of NaTPPMS and KTPPMS lack the needed solubility in water. Considering the water-solubilities of $(NH_4)_2SO_4$ (706 g/L 0°C) [12] *vs.* Na_2SO_4 (47.6 g/L 0°C) [12] aqueous ammonia was used to replace sodium hydroxide for the neutralization step in the TPPMS synthesis. Table I compares the literature synthesis and the method described herein. During neutralization with NH_3(aq), the temperature was held below 10°C. In our procedure precipitation commenced at a lower pH; initial precipitation occurred at pH 0 (pH paper range was 0–14 ± 1 pH unit). This is significant considering there is the potential for oxidation of the phosphine at higher pH values [13]. Neutralization was stopped at a pH between three and four to reduce the risk of oxide

TABLE I Comparison of TPPMS syntheses

Literature	*This Work*
20 g PPh_3 in 50 mL 20% fuming H_2SO_4	20 g PPh_3 in 50 mL 20% fuming H_2SO_4
Heated by boiling water bath for 75 min	Heated by boiling water bath for 70 min
Cooled, poured onto 400 g ice	Cooled, poured onto 300 g ice
Neutralized with 140/mL 50% NaOH(aq)	Neutralized with 120 mL NH_3(aq)
Separation of starting material	Filtered for ppt capture
Recrystallization	
Recrystallization	

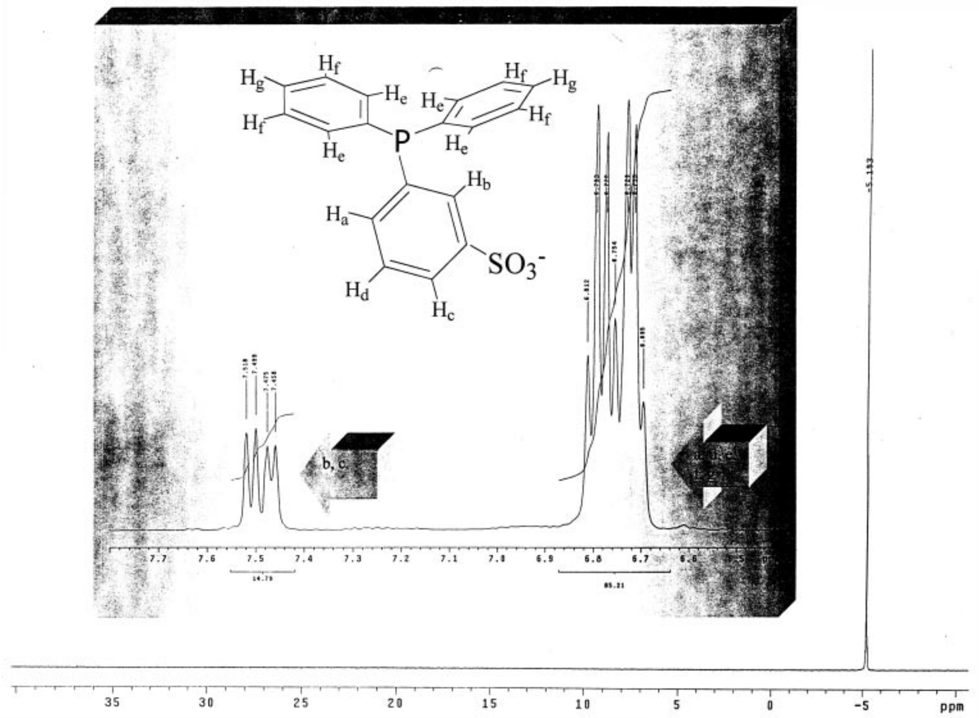

FIGURE 2 ^{31}P NMR and ^{1}H NMR (inset) of NH_4TPPMS.

formation. A few additional drops of base changes pH from four to above nine (where oxide product dominates) [14].

A ^{31}P NMR spectrum of the crude product indicated a trace amount of oxide, Fig. 2. The inset in Fig. 2 shows the aromatic region of the ^{1}H NMR. Integration of the ring protons (a–g) supports monosulfonation. The melting point of the raw, dried product was 224–228°C. DSC provided a melting onset of 226.8°C. Elemental analysis of the [NH_4]TPPMS ($C_{18}H_{18}O_3NPS$) provided the following results: Calculated: C 60.16, H 5.05, N 3.90. Found: C 59.87, H 5.17, N 3.88.

X-ray quality crystals were obtained by slow cooling of an aqueous solution over several days (stored in a Dewar flask). The resultant empirical formula for the crystal structure was determined to be $C_{18}H_{19}NPSO_{3.5}$ or $NH_4TPPMS \cdot ½H_2O$.

Using aqueous ammonia for the neutralization and reducing the amount of ice from 400 to 300 g generated a yield of 13.3 g (44.6%) *vs.* the published 5.7 g (21%) for NaTPPMS [11]. The increased concentration assisted precipitation. The filtrate contained NH_4TPPMS, $(NH_4)_2$TPPDS, $(NH_4)_3$TPPTS and mostly oxides. The solubility of NH_4TPPMS is 130 g/L at 24°C and increases to 360 g/L at 51°C.

The ammonium salt provides another route to the sodium salt as well as other salts because the solubility of the ammonium salt in H_2O is sufficiently large to produce a reasonable yield of NaTPPMS from a metathesis reaction.

$$Na_2SO_4(aq) + NH_4\,TPPMS(aq) \rightarrow NaTPPMS\ (s) + NH_4\,NaSO_4\ (aq) \qquad (1)$$

A saturated solution of Na_2SO_4, added slowly to a saturated solution of NH_4TPPMS, produces shiny flakes characteristic of NaTPPMS and uncharacteristic of NH_4TPPMS. The yield for the metathesis was 86%. Since the yield for NH_4TPPMS was 45%, this synthetic route produces an overall yield of 39% for NaTPPMS, a substantial improvement. A ^{31}P NMR of the dissolved precipitate indicated a single phosphorus resonance at − 5.5 ppm.

Metathesis was also used to prepare several transition metal salts, *i.e.*:

$$MnSO_4(aq) + 2NH_4TPPMS(aq) \rightarrow Mn(TPPMS)_2(s) + (NH_4)_2SO_4(aq) \qquad (2)$$

$$FeSO_4(aq) + 2NH_4TPPMS(aq) \rightarrow Fe(TPPMS)_2(s) + (NH_4)_2SO_4(aq) \qquad (3)$$

$$CoSO_4(aq) + 2NH_4TPPMS(aq) \rightarrow Co(TPPMS)_2(s) + (NH_4)_2SO_4(aq) \qquad (4)$$

$$NiSO_4(aq) + 2NH_4TPPMS(aq) \rightarrow Ni(TPPMS)_2(s) + (NH_4)_2SO_4(aq) \qquad (5)$$

For each methathetical reaction, the transition metal sulfate was added in approximately 20% excess of NH_4TPPMS. Table II presents the results of ^{31}P NMR spectral analysis and initial metathetical yield.

A series of complexes was made to compare the effect of transition metal cations on the coordinated ligand. Four equivalents of ligand were added to a suspension of $PtCl_2$ in D_2O to compare free and coordinated shifts. The water-soluble complex $(PtCl(TPPMS)_3)^+$ has two phosphorus resonances, a doublet for the phosphine ligands *trans* to each other and a triplet for the phosphine ligand *trans* to chloride. The fourth

TABLE II ^{31}P NMR shifts and metathetical yields of TPPMS species

Ligand	*^{31}P NMR shift* (ppm)	*Yield* (%)
NH_4TPPMS	-5.9^a	45^b
NaTPPMS	-5.5^a	86
$Mn(TPPMS)_2$	−1.3	93
$Fe(TPPMS)_2$	−1.5	91
$Co(TPPMS)_2$	−4.5	81
$Ni(TPPMS)_2$	−5.0	79

Solvent = DMSO referenced to H_3PO_4/D_2O external standard
[a] D_2O
[b] not metathetical.

equivalent of TPPMS was uncoordinated. Table III shows the cation effect was negligible on the coordinated ligands and modest on the uncoordinated ligand. The free ligand resonances are broadened, presumably from interaction with the paramagnetic metal ion.

A pH study was performed on the transition metal salt ligands dissolved in triply-distilled water under nitrogen. The concentration of each ligand was 4×10^{-3} M to limit hydrolysis. Table IV presents the results. However, some of the measurements were performed in air immediately after a nitrogen purge (second column). The values in the third column were measured under constant nitrogen purge. The small difference in the last two columns of Table IV arises from presence of CO_2. The pH of NH_4TPPMS under N_2 compares closely to theoretical as a salt with a nonhydrolyzing anion, e.g. NH_4Cl.

For a 4×10^{-3} M solution, the theoretical pH is 5.83. The solvated TPPMS transition metal cation acts as a weak Arrhenius acid lowering solution pH.

$$M^{2+}(aq) + 4H_2O(l) \rightleftharpoons M(OH)_2(aq) + 2H_3O^+(aq) \qquad (6)$$

Crystal Structure Analysis of NH_4TPPMS · ½H_2O Recrystallization from aqueous solution yielded colorless crystals of the solvated phosphine that were characterized by x-ray crystallographic analysis. Exposure of the crystals to air for a short time resulted in etching of the crystal surface. The structural representations are shown in Figs. 3 and 4 and crystallographic data and selected bond distances and angles are listed in Tables V and VI. Figures 3 and 4 show the asymmetric unit and

TABLE III $^{31}P\{^1H\}$ NMR shift (ppm) comparison: $PtCl_2 + 4$ equivalents of L in D_2O @ 50°C

L	*Tris Complex*[a] *(d)*	*(t)*	*Free ligand*
$Mn(TPPMS)_2$	23.2	12.4	− 4.7(b)
$Fe(TPPMS)_2$	23.1	12.3	− 2.8(b)
$Co(TPPMS)_2$	23.1	12.3	− 1.9(b)
$Ni(TPPMS)_2$	23.3	12.6	− 4.0(b)
NH_4TPPMS	23.3	12.6	− 5.2(s)

$(PtL_3Cl)^+$-*trans* $^1J_{P-Pt}$ 2500 Hz, -*cis* $^1J_{P-Pt}$ 3600 Hz, $^2J_{P-P}$ 18.7 Hz.
Referenced to H_4PO_4/D_2O external standard.

TABLE IV pH of 0.004 M L

L	*pH (in air after N_2 purge)*	*pH Under N_2*
H_2O		6.40
$Mn(TPPMS)_2$	5.75	
$Fe(TPPMS)_2$	5.12	
$Co(TPPMS)_2$	6.41	
$Ni(TPPMS)_2$	6.45	
NH_4TPPMS	5.72	5.80
NaTPPMS	5.78	6.02
Na_3TPPTS		5.95

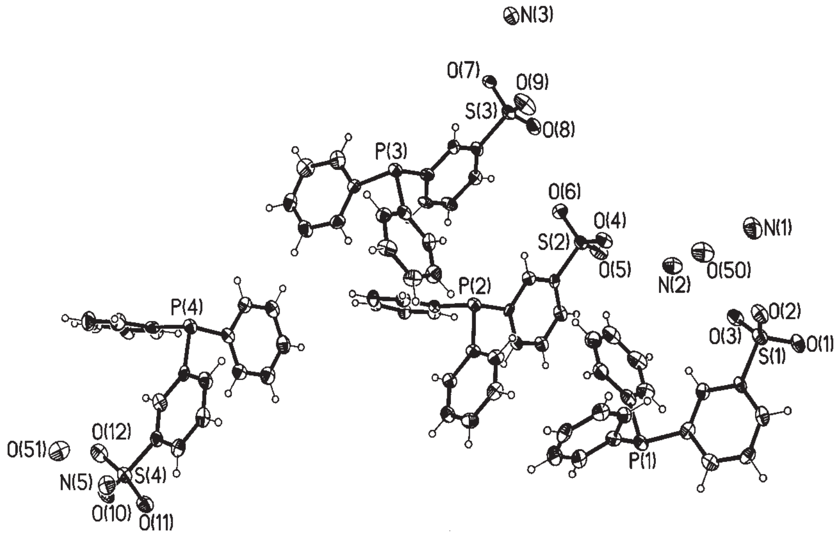

FIGURE 3 ORTEP plot of asymmetric unit in $NH_4TPPMS \cdot \frac{1}{2}H_2O$ structure. Thermal ellipsoids were drawn at 50% probabilities.

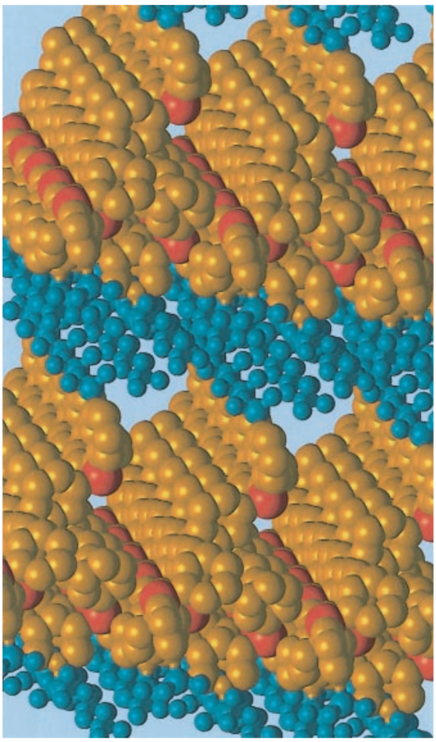

FIGURE 4 Packing arrangement of $NH_4TPPMS \cdot \frac{1}{2}H_2O$. Atoms in hydrophilic region are colored shades of green (N, O, & S), atoms in hydrophobic region are colored shaded of gold (C & P). The hydrogen atoms were omitted.

TABLE V Crystal data and structure refinement for $NH_4TPPMS \cdot ½H_2O$

Empirical formula	$C_{18}H_{19}NO_{3.50}PS$
Formula weight	368.37
Space group	P_1
Unit cell dimensions	
	$a = 10.3921(14)$ Å; $\alpha = 77.545(3)°$
	$b = 15.015$ (2) Å; $\beta = 85.539(2)°$
	$c = 23.905(3)$ Å; $\gamma = 89.997(3)°$
Volume	3630.8(9) $Å^3$
Z	8
Density (calculated)	1.348 $Mg\,m^{-3}$
Absorption coefficient	0.285 mm^{-1}
Temperature	90(1) K
Final R indices [$I > 2\sigma(I)$]	$R1 = 0.0807$, $wR2 = 0.1947$

TABLE VI Selected bond lengths (Å) and angles (°) for $NH_4TPPMS \cdot ½H_2O$

P(1)–C(75)	1.818(8)	C(75)–P(1)–C(83)	102.6(4)
P(1)–C(83)	1.823(9)	C(75)–P(1)–C(77)	101.8(3)
P(1)–C(77)	1.829(7)	C(83)–P(1)–C(77)	101.4(4)
S(1)–O(1)	1.446(5)	O(1)–S(1)–O(3)	113.1(3)
S(1)–O(3)	1.458(6)	O(1)–S(1)–O(2)	111.8(3)
S(1)–O(2)	1.470(5)	O(3)–S(1)–O(2)	111.8(3)
S(1)–C(79)	1.768(7)	O(1)–S(1)–C(79)	106.7(3)
C(75)–C(80)	1.397(10)	O(3)–S(1)–C(79)	105.7(3)
C(75)–C(78)	1.403(10)	O(2)–S(1)–C(79)	107.2(3)
C(76)–C(79)	1.401(10)	C(80)–C(75)–C(78)	118.2(7)
C(76)–C(77)	1.407(10)	C(80)–C(75)–P(1)	117.5(6)
C(77)–C(81)	1.377(11)	C(78)–C(75)–P(1)	124.4(6)
C(78)–C(82)	1.379(10)	C(79)–C(76)–C(77)	119.3(8)
C(79)–C(84)	1.376(11)	C(81)–C(77)–C(76)	118.4(7)
C(80)–C(88)	1.404(11)	C(81)–C(77)–P(1)	117.8(6)
C(81)–C(85)	1.408(10)	C(76)–C(77)–P(1)	123.8(6)
C(82)–C(89)	1.411(10)	C(82)–C(78)–C(75)	121.1(7)
C(83)–C(87)	1.396(12)	C(84)–C(79)–C(76)	121.2(7)
C(83)–C(90)	1.408(11)	C(84)–C(79)–S(1)	119.8(5)
C(84)–C(85)	1.383(10)	C(76)–C(79)–S(1)	119.0(7)
C(86)–C(90)	1.371(12)	C(75)–C(80)–C(88)	120.5(7)
C(86)–C(91)	1.375(13)	C(77)–C(81)–C(85)	122.3(7)
C(87)–C(92)	1.394(12)	C(78)–C(82)–C(89)	120.0(7)
C(88)–C(89)	1.361(10)	C(87)–C(83)–C(90)	117.4(8)
C(91)–C(92)	1.361(13)	C(87)–C(83)–P(1)	125.1(7)
C(89)–C(88)–C(80)	120.8(7)	C(90)–C(83)–P(1)	117.4(7)
C(88)–C(89)–C(82)	119.5(8)	C(79)–C(84)–C(85)	120.3(7)
C(86)–C(90)–C(83)	120.7(9)	C(84)–C(85)–C(81)	118.5(8)
C(92)–C(91)–C(86)	119.4(9)	C(90)–C(86)–C(91)	121.1(9)
C(91)–C(92)–C(87)	120.9(10)	C(92)–C(87)–C(83)	120.4(9)

the packing arrangement in the crystal, respectively. Figure 3 shows some interesting features with four formula units holding two water molecules in the asymmetric unit. The cation, water and anion spatial positioning creates four unique sulfonate groups. Although the hydrogen atoms were not located, hydrogen bonding can be inferred from oxygen and nitrogen positions. Typical hydrogen bond lengths to oxygen and nitrogen atoms average from 0.9 to 2.0 Å [15]. The oxygen of the first sulfonate group, is hydrogen bonded to a single ammonium ion, N(1)–O(2), 2.90(3) Å. The next sulfonate's oxygen is hydrogen bonded to an ammonium ion that is hydrogen bonded to water, O(4)–N(2), 2.81(9) Å, N(2)–O(50), 2.76(3) Å. The third sulfonate group has two oxygens close enough to hydrogen bond with an ammonium O(7)–N(3), 3.02(2) Å, O(9)–N(3), 3.12(9) Å). The last sulfonate group is hydrogen bonded to water, O(51)–O(12), 2.73(6) Å and ammonium ion, O(10)–N(5), 2.86(2) Å.

The packing arrangement driven by hydrogen bonding created hydrophilic and hydrophobic regions with an inversion point located in the center of the cell. For clarity, the atoms considered hydrophilic are colored shades of green (N, O & S) and the hydrophobic atoms are colored shades of gold (C & P). The hydrogen atoms were not drawn except for the ammonium cation to form the tetrahedral structure. This graphical style has been previously used in the literature [16]. A nickel atom was added to the phosphorus at a bond distance of 2.28 Å and the van der Waals radius of the atom that created the largest "semicone angle" was doubled permitting calculation of a cone angle from x-ray structural data [17]. A cone angle of 151.6° provides a comparison with the theoretical calculation of 151.9°.

Crystal Structure Analysis of Fe(TPPMS)$_2$·5H$_2$O Slowly cooling a boiling aqueous solution of Fe(TPPMS)$_2$ to room temperature in a Dewar flask produced yellow needles. The structural representations, unit cell and lattice, are shown in Figs. 5 and 6, respectively. Crystallographic data and selected bond distances and angles are listed in Tables VII and VIII. The asymmetric unit contains four TPPMS anions, two iron(II) cations and ten water molecules. Although all sulfonate groups are oriented toward iron, only two of the four sulfonate groups are attached to iron through oxygen while the other two anions are uncoordinated. The bond lengths for the two coordinated groups were 2.12(5) Å, O(17)–Fe(1) and 2.11(5) Å, O(2)–Fe(2). The uncoordinated sulfonates (closest oxygens to iron(II) are at distances of

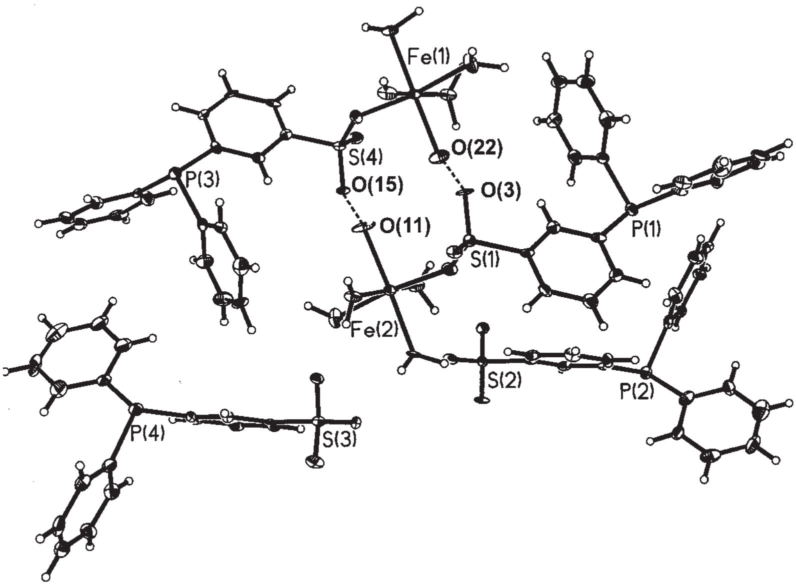

FIGURE 5 ORTEP plot of asymmetric unit in Fe(TPPMS)$_2$·5H$_2$O structure. Thermal ellipsoids were drawn at 50% probabilities.

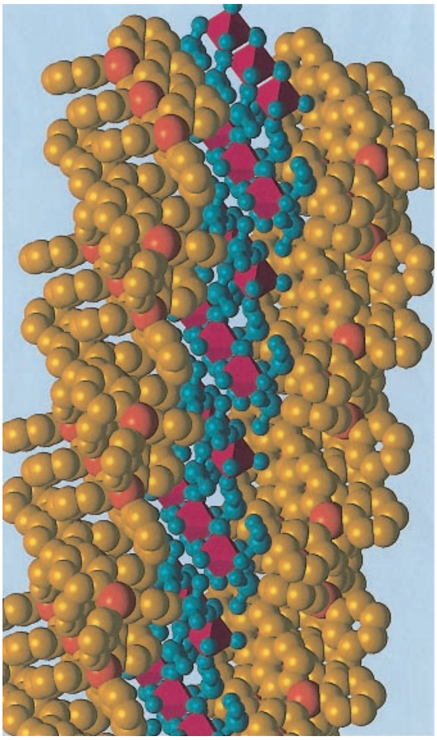

FIGURE 6 Packing arrangement of $Fe(TPPMS)_2 \cdot 5H_2O$. Atoms in hydrophilic region are colored shaded of green (N, O & S) and Fe is red, atoms in hydrophobic region are colored shades of gold (C & P). The hydrogen atoms were omitted.

TABLE VII Crystal data and structure refinement for $Fe(TPPMS)_2 \cdot 5H_2O$

Empirical formula	$C_{36}H_{38}FeO_{11}P_2S_2$
Formula weight	828.57
Space group	$P2_1$
Unit cell dimensions	
	$a = 6.3642(4)$ Å; $\alpha = 90°$
	$b = 48.313$ (3) Å; $\beta = 98.035(1)°$
	$c = 12.3321(7)$ Å; $\gamma = 90°$
Volume	3754.6(4) $Å^3$
Z	4
Density (calculated)	1.466 $Mg\,m^{-3}$
Absorption coefficient	0.657 mm^{-1}
Temperature	90(1) K
Final R indices [$I > 2\sigma(I)$]	$R1 = 0.0448$, $wR2 = 0.0929$

4.24(9) Å, O(14)–Fe(2) and 4.10(1) Å, O(5)–Fe(2). The remainder of the coordination sphere for the hexacoordinate iron(II) was occupied by water. Figure 5 also shows a possible 12-member ring formation through the two iron centers. The created bonds are drawn between O(11)–O(15), 2.74(5) Å and O(3)–O(22), 2.73(5) Å (there are 10 atoms shown plus the two hydrogen atoms) using dashed lines. The gold and green colored packing diagram in Fig. 6 shows the formation of hydrophilic and hydrophobic

TABLE VIII Bond lengths [Å] and angles [°] for $Fe(TPPMS)_2 \cdot 5H_2O$

Fe(1)–O(18)	2.085(6)	O(18)–Fe(1)–O(19)	171.9(2)
Fe(1)–O(19)	2.114(5)	O(18)–Fe(1)–O(22)	90.6(2)
Fe(1)–O(22)	2.106(5)	O(19)–Fe(1)–O(22)	86.7(2)
Fe(1)–O(17)	2.125(5)	O(18)–Fe(1)–O(17)	91.0(2)
Fe(1)–O(20)	2.129(5)	O(19)–Fe(1)–O(17)	96.8(2)
Fe(1)–O(21)	2.125(5)	O(22)–Fe(1)–O(17)	94.6(2)
S(4)–O(16)	1.461(4)	O(18)–Fe(1)–O(20)	87.9(2)
S(4)–O(15)	1.459(4)	O(19)–Fe(1)–O(20)	84.6(2)
S(4)–O(17)	1.457(5)	O(22)–Fe(1)–O(20)	91.7(2)
S(4)–C(6)	1.768(7)	O(17)–Fe(1)–O(20)	173.6(2)
P(3)–C(10)	1.837(7)	O(18)–Fe(1)–O(21)	90.6(2)
P(3)–C(16)	1.840(7)	O(19)–Fe(1)–O(21)	92.05(19)
P(3)–C(23)	1.842(6)	O(22)–Fe(1)–O(21)	178.7(2)
S(3)–O(13)	1.460(5)	O(17)–Fe(1)–O(21)	85.8(2)
S(3)–O(12)	1.465(4)	O(20)–Fe(1)–O(21)	87.9(2)
S(3)–O(14)	1.467(5)	O(16)–S(4)–O(15)	112.6(3)
S(3)–C(2)	1.773(7)	O(16)–S(4)–O(17)	113.0(3)
P(4)–C(58)	1.829(8)	O(15)–S(4)–O(17)	112.6(3)
P(4)–C(19)	1.831(7)	O(16)–S(4)–C(6)	106.9(3)
P(4)–C(12)	1.859(7)	O(15)–S(4)–C(6)	106.6(3)
C(58)–P(4)–C(19)	100.0(3)	O(17)–S(4)–C(6)	104.4(3)
C(58)–P(4)–C(12)	103.3(3)	O(13)–S(3)–O(14)	112.3(3)
C(19)–P(4)–C(12)	102.9(3)	O(12)–S(3)–O(14)	112.9(3)
C(10)–P(3)–C(16)	101.2(3)	O(13)–S(3)–C(2)	106.6(3)
C(10)–P(3)–C(23)	101.3(3)	O(12)–S(3)–C(2)	105.3(3)
C(16)–P(3)–C(23)	103.2(3)	O(14)–S(3)–C(2)	105.4(3)

moieties following the style of Fig. 4 with the additional color of red added to locate the transition metal which is drawn as an octahedron.

Structures of $Co(TPPMS)_2 \cdot 5H_2O$ and $Ni(TPPMS)_2 \cdot 7H_2O$: The packing arrangement of $Co(TPPMS)_2 \cdot 5H_2O$ and $Ni(TPPMS)_2 \cdot 7H_2O$, show similar hydrophobic and hydrophilic regions. The crystals grown from slow cooling were of poor quality and ultimately provided crystallographic data with R values of 14 and 16% for the Co(II) and Ni(II) salts, respectively. Crystallographic details are provided in the Supplementary Data.

CONCLUSION

The ammonium salt of TPPMS provides a simple higher yield route to NaTPPMS, and provides a route for incorporating a variety of transition metal cations with the water-soluble phosphine ligand. The complexes PtL_3Cl^+ show that the TPPMS retains coordination ability through phosphorus with the transition metal salts incorporated. The crystal structure determinations show distinct hydrophobic and hydrophilic regions; the hydrophilic regions are extensively hydrogen bonded while the hydrophobic regions exhibit π-stacking of the aromatic rings.

Acknowledgments

We are grateful to the Department of Energy, Basic Energy Sciences, Grant No, ER 13775 for support of this research. Stephanie Miller recorded the pH's listed in the first column of Table IV. Professor George Nancollas's group provided triply-distilled water. The use of Professor Phil Coppens x-ray diffraction equipment is gratefully acknowledged. MRB acknowledges a sabbatical from Erie Community College that enabled him to conduct this research.

SUPPORTING INFORMATION AVAILABLE

Supplementary information is available from the authors containing: (1) ^{31}P NMR to indicate purity of NH_4TPPTS and NaTPPTS, 3 pages, (2) oxidation of NH_4TPPTS and NaTPPTS, 2 pages, (3) crystal data and structure refinement for $NH_4TPPMS \cdot ½H_2O$, one page, (4) atomic coordinates for $NH_4TPPMS \cdot ½H_2O$, 2 pages, (5) bond lengths and angles for $NH_4TPPMS \cdot ½H_2O$, 3 pages, (6) anisotropic displacement parameters for $NH_4TPPMS \cdot ½H_2O$, 2 pages, (7) hydrogen coordinates for $NH_4TPPMS \cdot ½H_2O$, 2 pages, (8) crystal data and structure refinement for $Fe(TPPMS)_2 \cdot 5H_2O$, one page, (9) atomic coordinates for $Fe(TPPMS)_2 \cdot 5H_2O$, 2 pages, (10) bond lengths and angles for $Fe(TPPMS)_2 \cdot 5H_2O$, 2 pages, (11) anisotropic displacement parameters for $Fe(TPPMS)_2 \cdot 5H_2O$, 2 pages, (12) hydrogen coordinates for $Fe(TPPMS)_2 \cdot 5H_2O$, 2 pages, (13) crystal data for $Co(TPPMS)_2 \cdot 5H_2O$, one page, (14) atomic coordinates for $Co(TPPMS)_2 \cdot 5H_2O$, 3 pages, (15) bond lengths and angles for $Co(TPPMS)_2 \cdot 5H_2O$, 5 pages, (16) anisotropic displacement parameters for $Co(TPPMS)_2 \cdot 5H_2O$, one page, (17) crystal data for $Ni(TPPMS)_2 \cdot 7H_2O$, one page, (18) atomic coordinates for $Ni(TPPMS)_2 \cdot 7H_2O$, 2 pages, (19) bond lengths and angles for $Ni(TPPMS)_2 \cdot 7H_2O$, 2 pages.

References

[1] S. Ahrlad, S. Chatt, N.R. Davies and A.A. Williams (1958). *J. Chem. Soc.*, 276.
[2] E. Kuntz (June 20, 1975). German Patent 2,627,354.
[3] E. Kuntz (1987). CHEMTECH. **17**, 570.
[4] (a) W.L. Dressick, C. George, S.L. Brandow, T.L. Schull and D.A. Knight (2000). *J. Org. Chem.*, **65**, 5059. (b) B. Cornils and W.A. Herman (1996). *Applied Homogeneous Catalysis by Organometallic Complexes*. Wiley-VCH, Weinheim. (c) I.T. Horvath (1997). *J. Mol. Catal. A: Chem.*, **116**, Editorial. (d) T.L. Schull, J.C. Fettinger, D.A. Knight (1996). *Inorg. Chem.*, **35**, 6717. (e) P. Kalck and F. Monteil (1992). *Adv. Organomet. Chem.*, **34**, 219. (f) M. Barton and J.D. Atwood (1991). *J. Coord. Chem.*, **24**, 43. (g) W.A. Herrmann, J.A. Kulpe, J. Kellner, H. Riepl, H. Bahrmann and W. Konkol (1990). *Angew. Chem., Int. Ed. Engl.*, **29**, 391. (h) F. Joo and A. Benyei (1989). *J. Organmet. Chem.*, **C19**, 363. (i) M. Russell (1988). *Platinum Met. Rev.*, **32**, 179. (j) F. Joo and I. Toth (1980). *J. Mol. Catal.*, 369. (k) A. Borowski, D. Cole-Hamilton and G. Wilkinson (1977). *New J. Chem.*, **2**, 137.
[5] M.Y. Darensbourg (Ed.) (1998). *Inorganic Synthesis*. Vol. 32, Chapter 1. John Wiley & Sons Inc., NY.
[6] W.A. Herrmann, C.W. Kohlpaintner (1993). *Angew. Chem. Int. Ed. Engl.*, **32**, 1524.
[7] B. Salvesen and S. Bjerrum (1962). *Acta Chem. Scand*, **16**, 735.
[8] (a) C. Larpent, R. Dabard and H. Patin (1987). *Inorg. Chem.*, **26**, 2922. (b) C. Larpent, R. Dabard and H. Patin (1988). *New J. Chem.*, **12**, 907. (c) W.A. Herrmann, C.W. Kohlpaintner (1993). *Angew. Chem. Int. Ed. Engl.*, **32**, 1524.
[9] C.A. Tolman (1977). *Chem. Rev.*, **22**, 313.
[10] D.J. Darensbourg and C.J. Bischoff (1993). *Inorg. Chem.*, **32**, 47.
[11] F. Joo, S. Kovacs, A. Katho, A. Benyez, T. Decur and D.J. Darensbourg (1998). *Inorganic Syntheses*, **32**, 1.
[12] R.C. Weast (Ed.) (1982). CRC Handbook, 61st edn., pp. B-78, B-150. CRC Press, Boca Raton, FL.
[13] S. Hida, P.J. Roman, Jr., A.A. Bowden and J.D. Atwood (1998). *J. Coord. Chem.*, **43**, 345.
[14] P.A. McLaughlin and J.G. Verkade (1998). *Organometallics*, **17**, 5937.
[15] (a) M.C. Etter (1990). *Acc. Chem. Res.*, **23**, 120. (b) R. Taylor and O. Kennard (1984). *Acc. Chem. Res.*, **17**, 320.

[16] Z. Xu, Y.-H. Kiang, S. Lee, E.B. Lobkovsky, and N. Emmott (2000). *J. Am. Chem. Soc.*, **122**, 8376.
[17] T.L. Brown and K.J. Lee (1993). *Coord. Chem. Rev.*, **128**, 89.
[18] G.T. Kerr and A.E. Schweizer (1980). *Inorganic Synthesis*, **20**, 48.
[19] SMART Software Reference Manual, Bruker AXS, Madison, WI, 1998.
[20] SAINT Software Reference Manual, Bruker AXS, Madison, WI, 1998.
[21] G.M. Sheldrick (1997). SHELXTL NT Version 5.10. *Program for Solution and Refinement of Crystal Structures*. University of Göttingen, Germany.
[22] Weblab ViewerPro®, Version 4.0, Molecular Simulation Inc. 2000.